ISSN (Online): 2455-7838
SJIF Impact Factor (2017): 5.705

EPRA International Journal of

Research & Development

(IJRD)

Monthly Peer Reviewed & Indexed
International Online Journal

Volume: 3, Issue:11,November 2018

Published By :
EPRA Journals

SJIF Impact Factor: 5.705 Volume: 3 | Issue: 11 | November | 2018 ISSN: 2455-7838(Online)
EPRA International Journal of Research and Development (IJRD)

EFFECTS OF THERMAL STRATIFICATION ON MHD RADIATIVE NANOFLUID FLOW OVER NONLINEAR STRETCHING SHEET

P K Pattnaik
Department of Mathematics, College of Engg. and Technology, Bhubaneswar, 751029

S Jena
Faculty of Mathematics, Centurion Universityof Technology and Management, Odisha, India

N Mishra
Department of Mathematics, College of Engg. and Technology, Bhubaneswar, 751029

ABSTRACT

The effects of thermal stratification, thermal radiation, applied electric and magnetic fields, Joules heating and viscous dissipation are numerically studied on a boundary layer flow of electrical conducting nanofluid over a nonlinearly stretching sheet. The governing partial differential equations are converted to a couple of ordinary differential equations by incorporating suitable similarity transformations and are solved by using 4th order Runge-Kutta method with shooting technique. The electrical conducting nanofluid particle fraction is controlled on the boundary passively rather than actively. The effects of velocity, temperature, and nanoparticles concentration volume fraction with skin friction, heat transfer characteristics are examined graphically. It is noticed that the variable thickness enhances all the profiles i.e., fluid velocity, temperature, and nanoparticle concentration volume fraction. For increasing values of thermal stratification, the heat and mass transfer rate at the surface increases but reverse trend is occurred in case of fluid temperature. Electric field accelerates the nanofluid velocity which resolved the sticking effects caused by a magnetic field and so the fluid velocity gets suppressed. Radiative heat transfer and viscous dissipation are sensitive to an increase in the fluid temperature and thicker thermal boundary layer thickness. Comparison with published work is examined and presented due to excellent agreement.

KEYWORDS: *MHD nanofluid; Variable thickness; Thermal radiation; Similarity solution;Thermal stratification.*

Highlights:

1. MHD nanofluid due to stretching sheet with variable thickness with passively controlled.
2. A similarity transformation is used then solved by 4th order Runge-Kutta method with shooting technique.
3. Electric and magnetic fields are taken into account in velocity and energy analysis.
4. Combined effect of thermal stratification is examined.

Nomenclature

b, c, d	positive constants
B_0	uniform transverse magnetic field
B	applied magnetic field
C_{fx}	skin friction coefficient
c_p	specific heat constant
C_∞	ambient concentration
D_B	Brownian diffusion coefficient
D_T	thermophoresis diffusion coefficient
E_0	uniform electric field factor
E_1	electrical field parameter
E	applied electric field
E_c	Eckert number
f	dimensionless stream function
$\bar{J}$	Joule current
κ	thermal conductivity
L_e	Lewis number
M	magnetic field parameter
N_b	Brownian motion parameter
N_t	thermophoresis parameter
N_{ux}	local Nusselt number
P_r	Prandtl number
q_m	wall mass flux
q_r	radiative heat flux
q_w	wall heat flux
R_d	radiation parameter
Re_x	local Reynolds number
S_t	thermal stratification parameter
S_{hx}	local Sherwood number
T	temperature of the fluid
T_0	reference temperature
T_W	constant temperature at the wall
T_∞	ambient temperature
u, v	velocity component
$x-, y-$	direction component
$\bar{V}$	velocity fluid
V_W	wall mass transfer

Greek symbols

α	wall thickness parameter
α_f	base fluid thermal diffusivity
σ^*	Steffan-Boltzmann constant
σ	electrical conductivity
η	dimensionless similarity variable
μ	dynamic viscosity of the fluid
υ	kinematic viscosity of the fluid
ρ	density
ρ_p	particle density
ρ_f	density of the fluid
$(\rho c)_f$	heat capacity of the fluid
$(\rho c)_p$	heat capacity of a nanoparticle
ψ	stream function
C	concentration of the fluid
C_W	nanoparticle volume fraction
C_∞	nanoparticle volume fraction
θ	dimensionless temperature
ϕ	dimensionless concentration
τ	ratio between the effective heat transfer capacity and the heat capacity of the fluid
τ_w	surface shear stress

Subscripts

∞	condition at the free stream
W	condition at the wall/surface

1. INTRODUCTION

More recently, a new class of fluids known as nanofluids has drawn attentions of researchers in diverse areas of science and engineering technology as result of wide coverage of industrial applications of these fluids. This new innovation aims at enhancing the thermal conductivities and the convective heat transfer of fluids through suspensions of ultrafine nanoparticles in the base fluids [1]. Nanofluid is a mixture of an ultrafine nanoparticle of diameter less than 100nm dispersed in the conventional basic fluid namely water, toluene, ethylene, and oil. Some common metallic nanoparticles are copper, silver, silicon, aluminum, and titanium which tends to enhances the thermal conductivities and hence convective heat transfer rate of such fluids, which increases the energy transport strength and enactment [2-7]. Considering variable thickness due to flow, it has gained consideration due to widely advances recently in the area of engineering enhancement in the fields of mechanical, civil, architectural etc [8-10]. This is rooted in the innovative work of Fang et al. [11] against variable thickness using pure fluid. The surface medium of variable thickness have influential values and significant noticed in industrial and engineering processes. It aims at reducing the heaviness of supplementary component and enhance the operation of devices. Consequently, this drew the attention of various researchers [12-17] for flow behaviour against stretching sheet involving variable thickness. The study of nanofluids with effects of magnetic fields has enormous applications in the fields of metallurgy and engineering advancement [18-30]. Such significant are derived in stretching of plastic sheets, polymer industry and metallurgy by hydromagnetic. In the area of metallurgical processes which involves cooling of continuous strips/filaments through drawing them from nanofluid [31]. Drawing these strips involves stretched at some point in time and also annealing and thinning of copper wires [32]. In these process, the desired properties of final product strongly depend by the virtue on the level of cooling from side to side drawing such strips in an electrically conducting fluid with impacts of magnetic fields [33]. Nanofluids are primarily aimed at cooling devices in the computer (cooling of microchips) and electronics devices (microfluidic) applications. Investigation showed that nanofluids with the influence of magnetic field, by varying the electromagnetic field, it absorbs energy and gives a controllable hyperthermia, which acts as super-para-magnetic fluid see the works of [34]. In different flows of practical relevance in nature as well as in many engineering devices, the environment is thermally stratified [35]. Stratification is a formation or deposition of layers which occur as results of temperature difference or variations of densities or due to the presence of different fluids. The discharge of hot fluid into enclosed regions more often leads in a stable thermal stratification containing lighter fluid overlying denser fluid [36]. The level at which these objects are cooled a vital bearing in mind on the desired properties of the finished product. These applications involve heat rejection into the environment namely lakes, seas, and rivers; thermal energy storage systems like solar ponds; and heat transfer through thermal sources namely condensers of power plants [37-39]. Related works pointed out that thermal stratification effects in electrical magnetohydrodynamic (MHD) boundary layer stretched flow of revised nanofluid model [40] containing nanoparticles with water base fluid due to variable thickness is not investigated yet. Pattnaik et al. [41-45] studied the behaviour of MHD fluid flow and observed some interesting results. Consequently, our main goal here is four folds. Firstly to examine thermal stratification effects through the heat in the magnetohydrodynamic (MHD) flow. Secondly to analyse electric field impact. Thirdly to address thermal radiation and Joule heating in view of Heat transfer phenomenon. Fourth to present formulation in the company of Brownian motion and thermophoresis. In manufacturing processes, the raw material passes through the die for the extrusion in a liquefied state under high temperature, with densities gradient leads to thermal stratification. Moving surface into a cooling medium is a mathematical tool for the process of heat treatment in the fields of engineering technology noticed in mechanical, civil, architectural involved variable thickness. The governing mathematical system which is partial differential equations is converted to a system of nonlinear coupled of ordinary differential equations by similarity transformation techniques. The resulted non-dimensional nonlinear convective effect are solved using implicit finite difference. Behaviours of various pertinent parameters on the velocity, temperature, and nanoparticle concentration are examined. Skin friction coefficient and Nusselt number are compared and analysed. A comparative assessment of the present and previous data is made with judgment.

2. MATHEMATICAL FORMULATION

We have considered a steady two-dimensional flow of magnetohydrodynamic (MHD) nanofluid due to a nonlinear stretching sheet with variable thickness. The velocity of the stretching sheet is denoted as $U_W(x)$ and the surface is taken at $y = A_1(x+b)^{(1-n)/2}$ as the nonlinear stretching surface variable, in which for $n=1$ the stretching sheet is of the same thickness. The boundary layer equations of the fluid flow are consist of the continuity equation, the momentum equation, energy equation and concentration equation. The laminar incompressible flow of viscous nanofluid in the presence of applied magnetic field $\mathbf{B}$ and electric field E are taken into consideration. The flow is due to stretching of a sheet from a slot through two equal and opposite force and thermally radiative. The magnetic and electric fields obey the Ohm's law define $\bar{J} = \sigma(\bar{E} + \bar{V} \times \bar{B})$. The magnetic field strength $B(x)$ and electric field $E(x)$ strength is applied normal to the flow field. The induced magnetic field is so small, so the induced magnetic field and Hall current impacts are insignificant. We choose the Cartesian coordinate system such that and are the velocity components of the fluid in the $x-$ and $y-$direction see Fig.1. The combined effects of thermal radiation, viscous dissipation, magnetic and electrical fields are incorporated. The nanofluid flow due to a nonlinear stretching sheet with variable thickness is considered. The investigation of the nanofluid which involves particles and liquid.

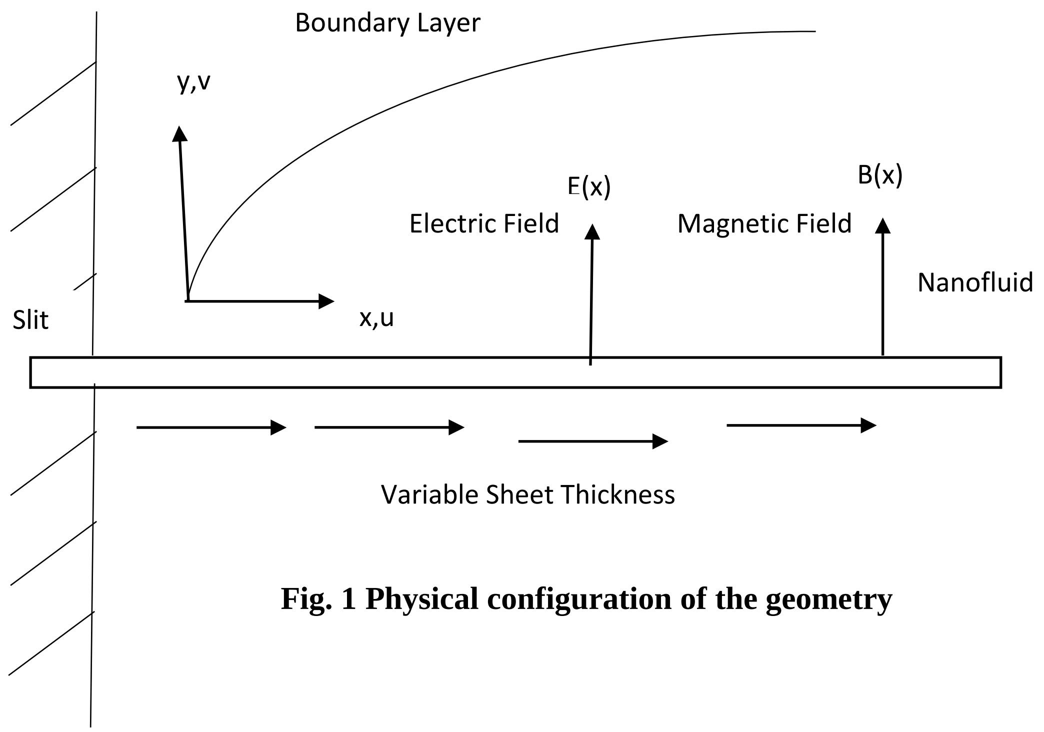

Fig. 1 Physical configuration of the geometry

The magnetohydrodynamic (MHD) boundary layer flow equation of an incompressible nanofluid are given as:

$$\frac{\partial u}{\partial x}+\frac{\partial v}{\partial y}=0 \tag{1}$$

$x-$ direction momentum equation

$$u\frac{\partial u}{\partial x}+v\frac{\partial u}{\partial y}=\frac{-1}{\rho_f}\frac{\partial P}{\partial x}+v\left(\frac{\partial^2 u}{\partial x^2}+\frac{\partial^2 u}{\partial y^2}\right)-\frac{\sigma}{\rho_f}\left(E(x)B(x)-B^2(x)u\right) \tag{2}$$

$y-$ direction momentum equation

$$u\frac{\partial v}{\partial x}+v\frac{\partial v}{\partial y}=\frac{-1}{\rho_f}\frac{\partial P}{\partial y}+v\left(\frac{\partial^2 v}{\partial x^2}+\frac{\partial^2 v}{\partial y^2}\right)-\frac{\sigma}{\rho_f}\left(E(x)B(x)-B^2(x)v\right) \tag{3}$$

$$\begin{aligned}u\frac{\partial T}{\partial x}+v\frac{\partial T}{\partial y}=&\frac{k}{\rho c_p}\left(\frac{\partial^2 T}{\partial x^2}+\frac{\partial^2 T}{\partial y^2}\right)+\tau\left[D_B\left(\frac{\partial C}{\partial x}\frac{\partial T}{\partial x}+\frac{\partial C}{\partial y}\frac{\partial T}{\partial y}\right)+\left(\frac{D_T}{T_\infty}\right)\left[\left(\frac{\partial T}{\partial x}\right)^2+\left(\frac{\partial T}{\partial y}\right)^2\right]\right]\\&-\frac{1}{\rho c_p}\frac{\partial q_r}{\partial y}+\frac{\mu}{\rho c_p}\left(\frac{\partial u}{\partial y}\right)^2+\frac{\sigma}{\rho c_p}(uB(x)-E(x))^2\end{aligned} \tag{4}$$

$$u\frac{\partial C}{\partial x}+v\frac{\partial C}{\partial y}=D_B\left(\frac{\partial^2 C}{\partial x^2}+\frac{\partial^2 C}{\partial y^2}\right)+\frac{D_T}{T_\infty}\left(\frac{\partial^2 T}{\partial x^2}+\frac{\partial^2 T}{\partial y^2}\right) \tag{5}$$

where $E(x)=E_0(x+b)^{(n-1)/2}, B(x)=B_0(x+b)^{(n-1)/2}$.

Corresponding boundary conditions [46]:

For $y=A_1(x+b)^{(1-n)/2}$,

$$u=U_W(x)=U_0(x+b)^n, v=0, T=T_W(x)=T_0+c(x+b)^n, D_B\frac{\partial C}{\partial y}+\left(\frac{D_T}{T_\infty}\right)\frac{\partial T}{\partial y}=0$$

For $y\to\infty, u\to 0, T\to T_\infty=T_0+d(x+b)^n, C\to C_\infty$ (6)

Using an order magnitude analysis of the $y-$direction momentum equation (3) (normal to the stretching sheet) and applying the normal boundary layer equation:

$$u>>v, \frac{\partial u}{\partial y}>>\frac{\partial u}{\partial x},\frac{\partial v}{\partial x},\frac{\partial v}{\partial y}$$

and $\frac{\partial P}{\partial y}=0$

To obtain similarity solution, the nondimensionalized variables are presented as [47-49]:

$$\psi=\left(\frac{2}{n+1}\nu U_0(x+b)^n\right)^{1/2}F(\xi), \xi=y\left(\frac{n+1}{2\nu}U_0(x+b)^{n-1}\right)^{1/2}, \phi(\eta)=\frac{(C-C_\infty)}{C_\infty}, \theta(\eta)=\frac{(T-T_\infty)}{(T_W-T_\infty)},$$

$$u=U_0(x+b)^nF(\xi), v=-\left(\frac{n+1}{2\nu}U_0(x+b)^{n-1}\right)^{1/2}\left(F(\xi)+\xi\left(\frac{n-1}{n+1}\right)F'(\xi)\right). \tag{7}$$

Substituting equation (7) into (1)-(3), we obtained the transformed ordinary differential equation as:

$$F'''(\xi)+F(\xi)F''(\xi)-\left(\frac{2n}{n+1}\right)(F'(\xi))^2+M(E_1-F'(\xi))=0 \tag{8}$$

The transformed boundary conditions are presented as:

$$\xi=0, F(\xi)=\alpha\frac{1-n}{1+n}, F'(\xi)=1$$

$$\xi\to\infty, F'(\xi)=0$$

where $\alpha=A_1\left(\frac{(n+1)}{2}\frac{U_0}{\upsilon}\right)^{1/2}$

Taking $F(\xi)=F(\xi-\alpha)=f(\eta)$ in equation (8) we get,

$$f'''(\eta)+f(\eta)f''(\eta)-\left(\frac{2n}{n+1}\right)(f'(\eta))^2+M(E_1-f'(\eta))=0 \tag{9}$$

Using the Rosseland approximation, the radiative heat flux is given by (Brewster [50])

$$q_r=-\frac{4\sigma^*}{3k^*}\frac{\partial T^4}{\partial y} \text{ where } T^4=4T_\infty^3T-3T_\infty^4$$

$$\frac{\partial q_r}{\partial y}=-\frac{16T_\infty^3\sigma^*}{3k^*}\frac{\partial^2 T}{\partial y^2}$$

So from equation (4),

$$u\frac{\partial T}{\partial x}+v\frac{\partial T}{\partial y}=\frac{k}{\rho c_p}\left(\frac{\partial^2 T}{\partial x^2}+\frac{\partial^2 T}{\partial y^2}\right)+\tau\left[D_B\left(\frac{\partial C}{\partial x}\frac{\partial T}{\partial x}+\frac{\partial C}{\partial y}\frac{\partial T}{\partial y}\right)+\left(\frac{D_T}{T_\infty}\right)\left[\left(\frac{\partial T}{\partial x}\right)^2+\left(\frac{\partial T}{\partial y}\right)^2\right]\right]$$

$$+\frac{1}{\rho c_p}\frac{16T_\infty^3\sigma^*}{3k^*}\frac{\partial^2 T}{\partial y^2}+\frac{\mu}{\rho c_p}\left(\frac{\partial u}{\partial y}\right)^2+\frac{\sigma}{\rho c_p}(uB(x)-E(x))^2$$

The transformed energy equation:

$$\frac{1}{P_r}\left(1+\frac{4}{3}R_d\right)\theta''+f\theta'-\frac{2}{n+1}f'\theta+N_b\theta'\phi'+N_t\theta'^2+E_c(f'')^2+ME_c(f'-E_1)^2-\frac{2n}{n+1}S_t f'=0 \quad (10)$$

The volume fraction concentration equation reduced to:

$$\phi''+\frac{N_t}{N_b}\theta''+L_e f\phi'=0 \quad (11)$$

The corresponding boundary conditions are:

$$f(0)=\alpha\frac{1-n}{1+n},\ f'(0)=1,\theta(0)=1-S_t,\ N_b\phi'(0)+N_t\theta'(0)=0$$
$$f'(\infty)\to 0,\quad \phi(\infty)\to 0,\quad \theta(\infty)\to 0. \quad (12)$$

where $M=\frac{2\sigma B_0^2}{\rho_f U_0(n+1)}, E_1=\frac{E_0}{U_0B_0(x+b)^n}, P_r=\frac{\mu c_p}{k}, \alpha=\frac{k}{\rho c_p}, \tau=\frac{(\rho c)_p}{(\rho c)_f}, S_t=\frac{c}{d}$

$$N_t=\frac{\tau D_T(T_w-T_\infty)}{vT_\infty}, N_b=\frac{\tau D_B\varphi_\infty}{v}, E_c=\frac{U_W^2(T_w-T_\infty)}{c_p}, R_d=\frac{4T_\infty^3\sigma^*}{k^*\kappa}, L_e=\frac{\alpha_f}{D_B}.$$

Physical quantities:

The skin friction coefficient is defined in terms of shear stress and density:

$$C_{fx}=\frac{\tau_w}{\rho U_w^2(x)}, \tau_w=\mu\left(\frac{\partial u}{\partial y}\right)_{y=A_1(x+b)^{(1-n)/2}}$$

Nusselt number is defined as:

$$N_{ux}=\frac{(x+b)^{\frac{1-n}{2}}}{\kappa(T_w-T_\infty)}q_w,\ q_w=-\left(\kappa+\frac{16\sigma^*}{3k^*}\right)\left(\frac{\partial T}{\partial y}\right)_{y=A_1(x+b)^{(1-n)/2}}$$

The Sherwood number is defined as:

$$S_{hx}=\frac{(x+b)^{\frac{1-n}{2}}}{D_B\varphi_\infty}q_m,\ q_m=-D_B\left(\frac{\partial C}{\partial y}\right)_{y=A_1(x+b)^{(1-n)/2}}$$

Non-dimensional form of the above quantities are:

$$C_{fx}\sqrt{\mathrm{Re}_x}=\sqrt{\frac{1+n}{2}}f''(0), N_{ux}/\sqrt{\mathrm{Re}_x}=-\left(1+\frac{4}{3}R_d\right)\sqrt{\frac{1+n}{2}}\theta'(0), S_{hx}/\sqrt{\mathrm{Re}_x}=-\sqrt{\frac{1+n}{2}}\phi'(0) \quad (13)$$

where $\mathrm{Re}_x=\frac{A_1(x+b)^{(n+1)}}{v}=\frac{U_w(x+b)}{v}$.

RESULTS AND DISCUSSION

The set of nonlinear highly ordinary differential equations (9), (10), (11) with the respective boundary conditions (12) are solved numerically using Keller box method [51], for the velocity, temperature and concentration fields. The computation is repeated until some convergence criterion is satisfied up to the desired accuracy of a 10^{-5} level. Comparison with the existing results published by Fang et al. [11] shows a perfect agreement. In the present computation the value of the pertinent parameters are considered as $M = n = P_r = E_c = R_d = L_e = 1$ $E_1 = S_t = N_t = N_b = 0.1$unless otherwise stated.

Figs. 2(a-c) displayed the dimensionless velocity fields for various values of magnetic field parameter $'M'$, electric field parameter$'E_1'$ and nonlinear stretching sheet parameter$'n'$. Variation in velocity with an increase in magnetic field parameter with effects of variable thickness can be seen from Fig. 2(a). It is noticed that an increase in$'M'$, the velocity profiles reduced close to the wall and suddenly increase near the stretching sheet surface as result of electrical force. The Lorentz force which acts as a retarding force tends to enhance the frictional resistance opposing the nanofluid movement in the hydrodynamic boundary layer thickness. In the case of presence of variable thickness, the velocity and momentum boundary layer is higher. The effect of electric field parameter on the velocity profiles is presented in Fig. 2(b) with effects of variable thickness. Increasing in the values of$'E_1'$ accelerate the nanofluid flow more significantly near the stretching sheet surface with thicker hydrodynamic boundary layer thickness. This is as result of Lorentz force that is arising due to an electrical force acting as accelerating force which tends to reduce the frictional resistance leading to shifting the stream away from the nonlinear stretching sheet. The velocity increase as the momentum boundary layer becomes thicker in the presence of variable thickness parameter to that of absence. Fig. 3(c) portrays the influence of nonlinear stretching sheet parameter $'n'$ in the presence of electric field parameter ($E_1 = 0.1$) and absence ($E_1 = 0$). Higher values of resulted in an increase in the velocity profiles and thicker momentum boundary layer thickness. In the case of presence of electric field, the flow shifts away from the stretching surface at initial stage with an increase in the velocity field. The velocity gradient reduced as the nonlinear stretching sheet rises.

The variation of temperature field $\theta(\eta)$ for various values of Prandtl number$\mathrm{P_r}$, thermal radiation parameterR_d, Eckert numberE_c and thermal stratification parameterS_t is investigated in the Figs 3(a-d). From Fig. 3(a), we examined that for larger momentum boundary layer thickness is greater than thermal boundary layer thickness with thicker thermal boundary layer thickness with a presence of variable thickness. Since Prandtl number is the momentum diffusivity to thermal diffusivity. The fluid temperature decreases close to the nonlinear stretching sheet surface significantly for an increase in the values of Prandtl number. The rate of heat transfer at the surface increase with increase in values of$\mathrm{P_r}$. Radiation impacts on the temperature field is depicted in Fig. 3(b). An increase in values of R_d enhances the heat flux from the nonlinear stretching sheet which resulted in an increase in the fluid's temperature. Hence the temperature field and thermal boundary layer increase with an increase inR_d. In the absence of variable thickness, the thermal boundary layer thickness is lower compared to presence. The temperature gradient reduced for higher values of thermal radiation. Fig. 3(c) illustrate that temperature is an increasing function of the Eckert number E_c. The fluid temperature and thermal boundary layer thickness increase significantly in the presence of variable thickness. Eckert number is the ratio of kinetic energy to enthalpy. For higher values ofE_c, kinetic energy rises with consequently enhances the nanofluid temperature. The rate of heat transfer at the surface reduced for much quantity of viscous dissipation. Fig. 3(d) is sketched to analyse the variation in temperature field for varying thermal stratification parameterS_t. It is worth notice that fluid temperature is a decreasing function of thermal stratification with a rise in variable thickness parameter. The effective convective potential that coexists between the nonlinear stretching sheet and the ambient nanofluid decreased with an increase inS_t . In view of this, the fluid temperature and thermal boundary layer thickness reduced for higher thermal stratification. The rate of heat transfer at the surface increases for an increase in the amount of thermal stratification. Figs. 4(a-d) are plotted to examine the behaviour of Brownian motion parameter N_b, thermophoresis parameter N_t, Lewis number L_e and Prandtl number $\mathrm{P_r}$ on the dimensionless nanoparticles concentration field $\phi(\eta)$. From Fig. 4(a), it is obvious that the nanoparticle concentration and its solutal boundary layer thickness is smaller for larger Brownian motion parameter with thicker concentration boundary layer as resulted of variable thickness. The nanoparticle concentration gradient at the boundary wall is controlled passively at the surface by the expression of $\left(-N_t/N_b\right)$ and temperature gradient. The effects of thermophoresis parameter on the concentration profile $\phi(\eta)$ is demonstrated in Fig. 4(b). It is noticed that the nanoparticle concentration increases with an increase in thermophoresis parameter and higher with variable thickness. This is as result of thermophoresis force developed by the rate of mass transfer at the surface creates a smooth flow far from the nonlinear stretching sheet surface. In view of this more heated fluid shift away from the surface and hence with much amount of thermophoresis, the fast flow from the nonlinear stretching sheet due to the presence of thermophoresis force resulting to enhancement in the nanoparticle concentration boundary layer thickness. The influence of Lewis number L_e on nanoparticle concentration is revealed in Fig. 4(c). It is worth noticing that the nanoparticle concentration reduced significantly with higher values of Lewis number but thicker with variable thickness. This reduction in nanoparticle concentration and solutal boundary layer thickness is as results of the change in Brownian diffusion coefficient. It noted that higher values Lewis number associated to weaker Brownian diffusion coefficient. The concentration gradient increases with higher values of Lewis number. Fig. 4(d) shows the variation of Prandtl number $\mathrm{P_r}$ on concentration profile $\phi(\eta)$. An obvious observation is marked i.e., for increasing values of $\mathrm{P_r}$, concentration profile is enhanced.

Fig. 5(a-d) shows the variation of Skin friction coefficient. It is clear that, Skin friction coefficient increases by increasing $M, \alpha \,\&\, n$ while it decreases for higher values E_1 and for $M \,\&\, \alpha, 0 < \eta < 1$, it also decreases. From Figs. (6) and (7) it is remarked that, Local Nusselt number increases for higher values of $N_t, N_b, E_1, P_r \,\&\, n$ however it decreases for higher values of M, R_d, E_c and S_t. From Figs. (8), it is observed that Sherwood number increases for higher values of L_e, N_b, R_d and S_t however it decreases for higher values of N_t and P_r.

3. CONCLUSION

The impact of thermal radiation and Joule heating due to the magnetohydrodynamic (MHD) flow of nanofluid against a nonlinearly stretching sheet with variable thickness are examined in the presence of thermal stratification. Thermal stratification and passively controlled nanoparticle concentration on the boundary condition in the presence of applied magnetics and electric fields makes this investigation novelone.

The main conclusion of this study is stated as follows:

i. High velocity is obtained for higher values of electric field and nonlinear stretching sheet.
ii. The temperature reduces with increasing values of the thermal stratification parameter and Prandtl number.
iii. Magnetic field effects on electrical conducting nanofluid suppressed the flow at the initial stage and after some distance enhances due to electrical force near the nonlinear stretching sheet surface which leads to enhancement of the skin friction coefficient.

iv. The radiative heat transfer and viscous dissipation in the presence of variable thickness plays a dominant role in the temperature of the nanofluid.

v. Lewis number and thermophoresis of nanoparticles reduces the nanoparticle concentration volume fraction for higher values but enhanced the mass transfer rate at the controlled surface.

vi. Brownian movement and thermophoresis nanoparticle deposition in the presence of variable thickness and electric field reaches a significant role on the nanoparticle concentration volume fraction due to random movement of ultrafine nanoparticle suspended in the base fluid with passively controlled boundary at the wall.

Fig.2 Variation of velocity profile f`(η)

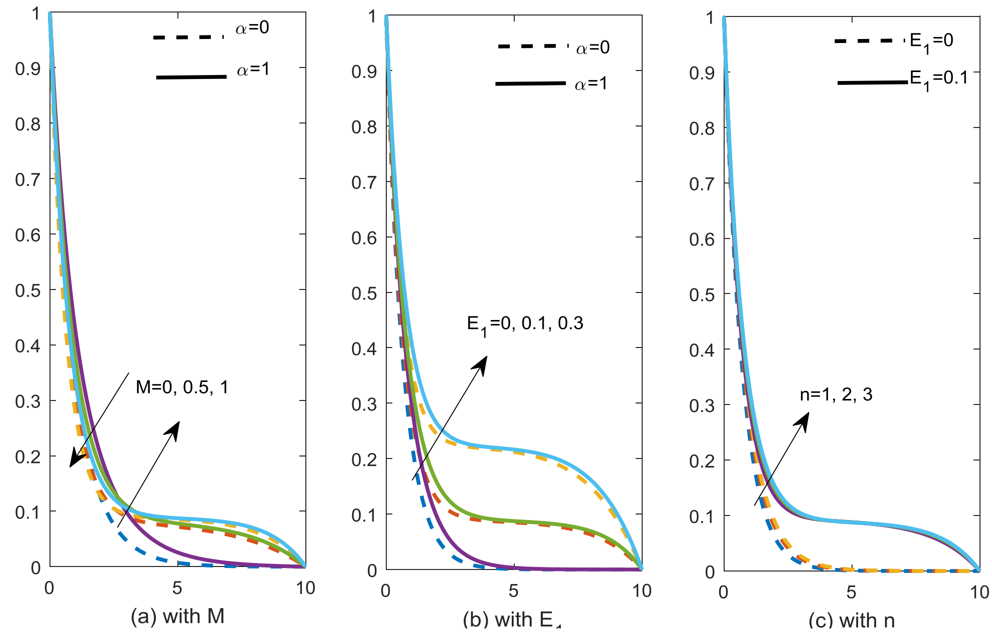

Fig.3 Variation of Temperature profile $\theta(\eta)$

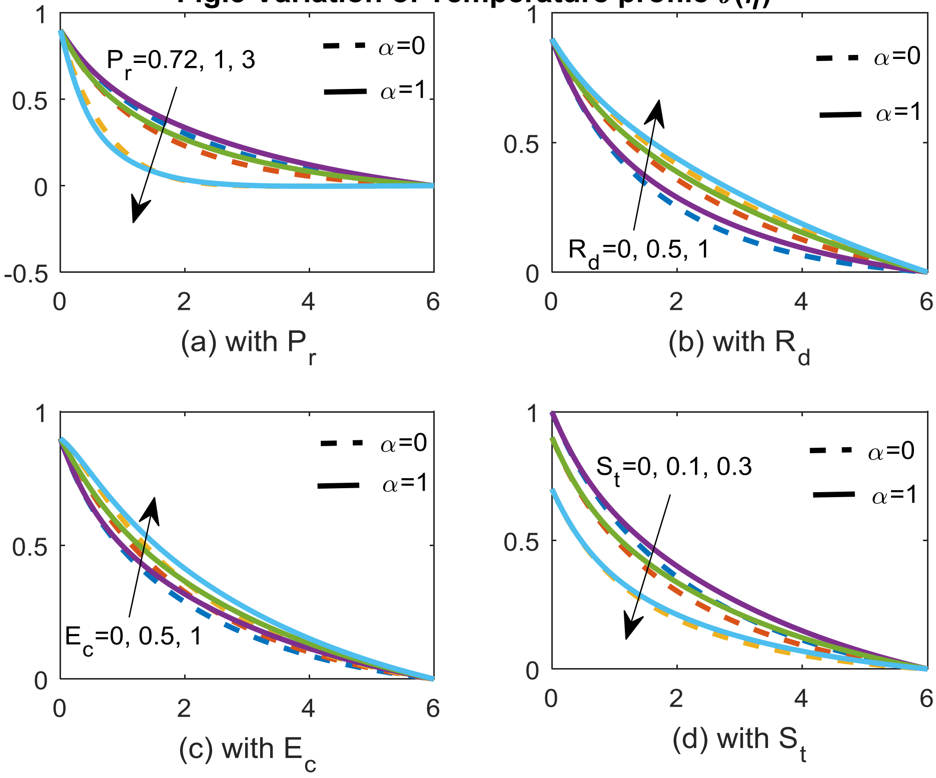

Fig.4 Variation of Concentration profile $\phi(\eta)$

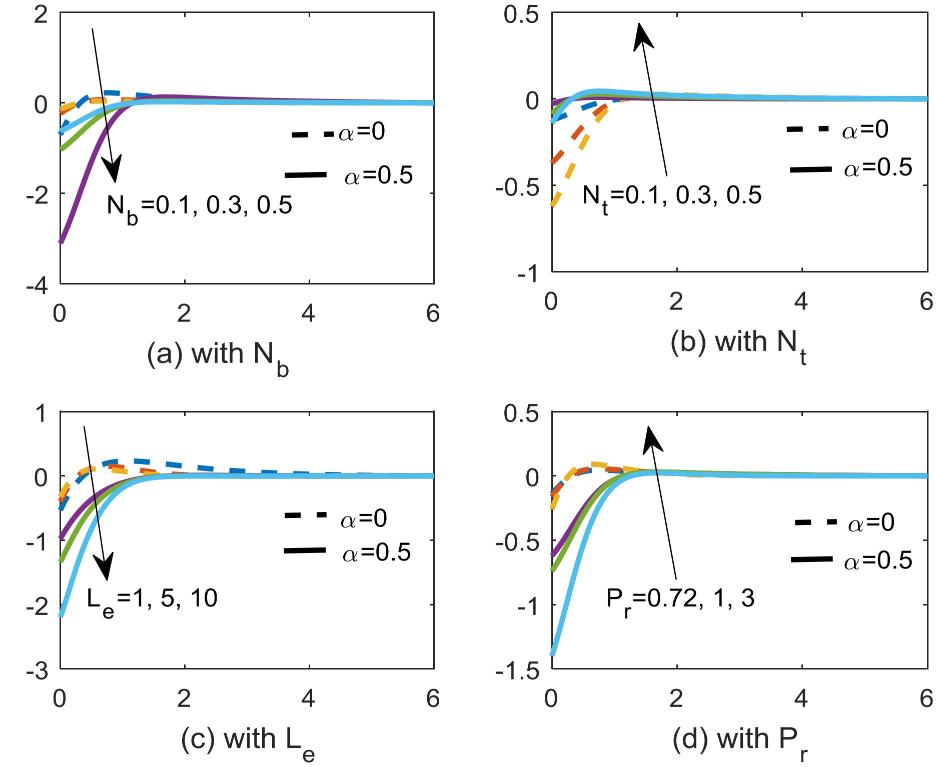

Fig.5 Variation of Skin Friction Coefficient C_f

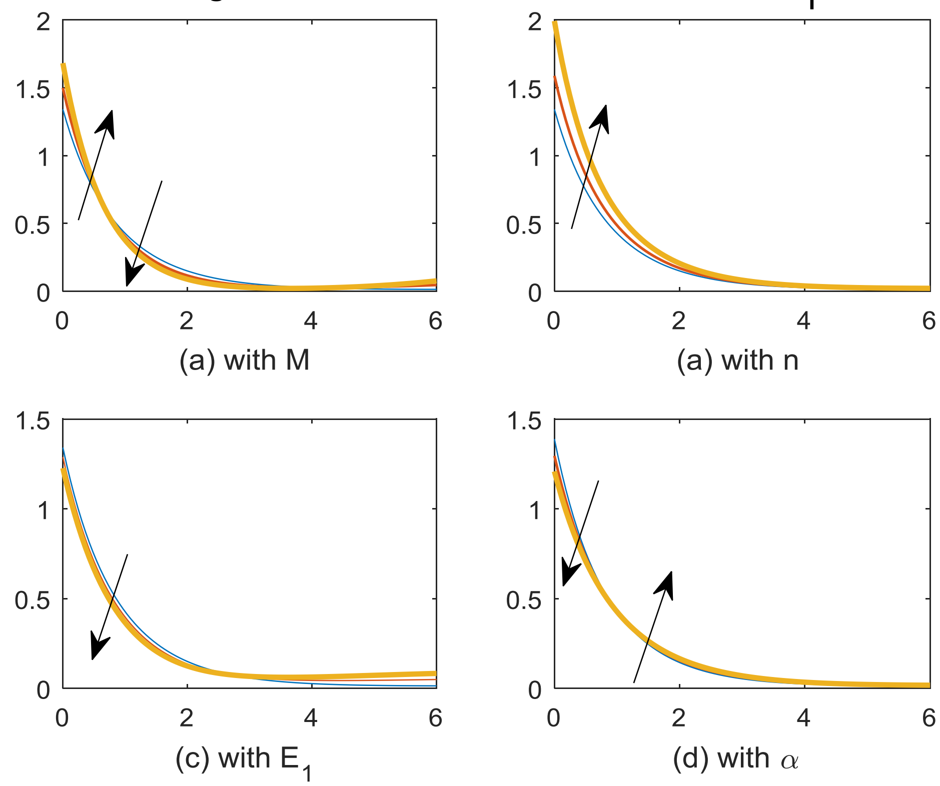

Fig.6 Variation of Local Nusselt Number Nu_x

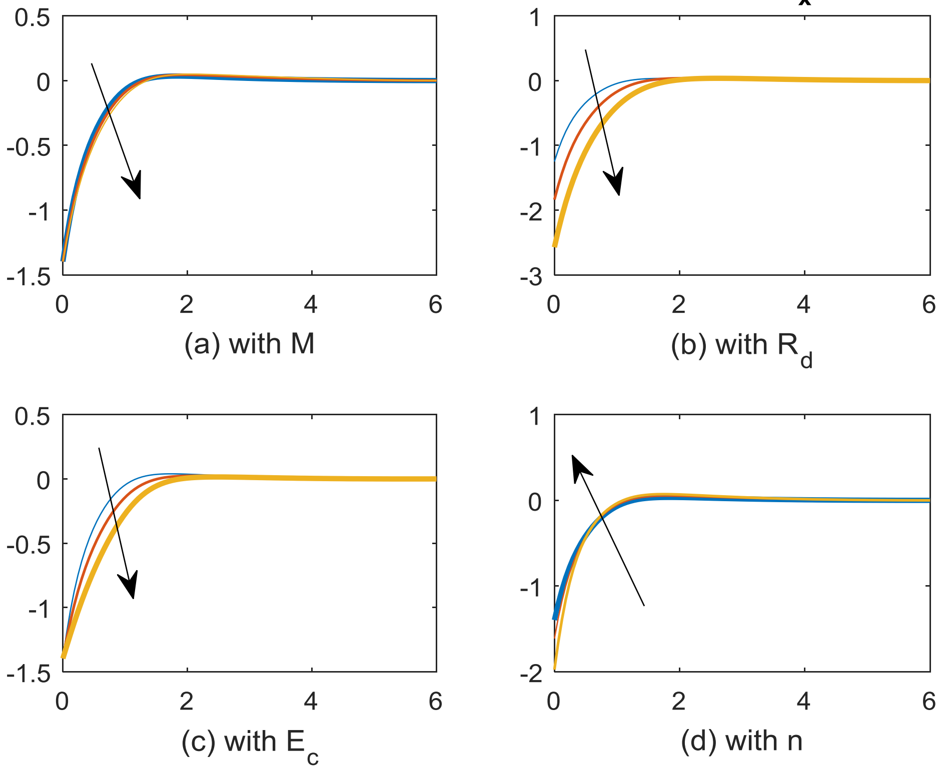

Fig.7 Variation of Local Nusselt Number Nu_x

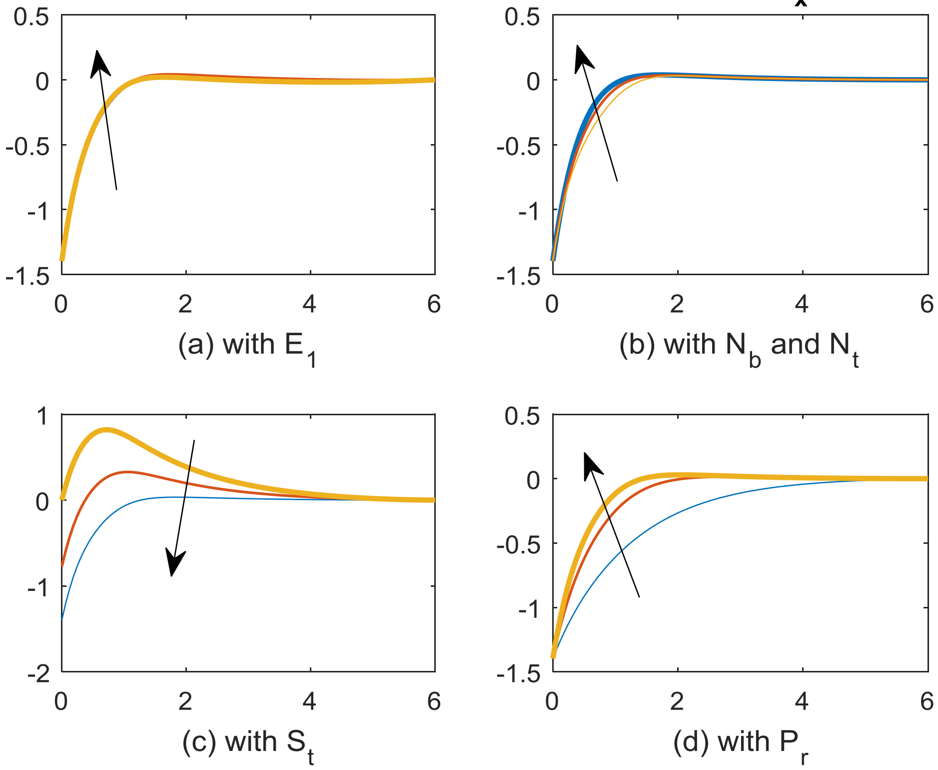

Fig.8 Variation of Sherwood Number Sh_x

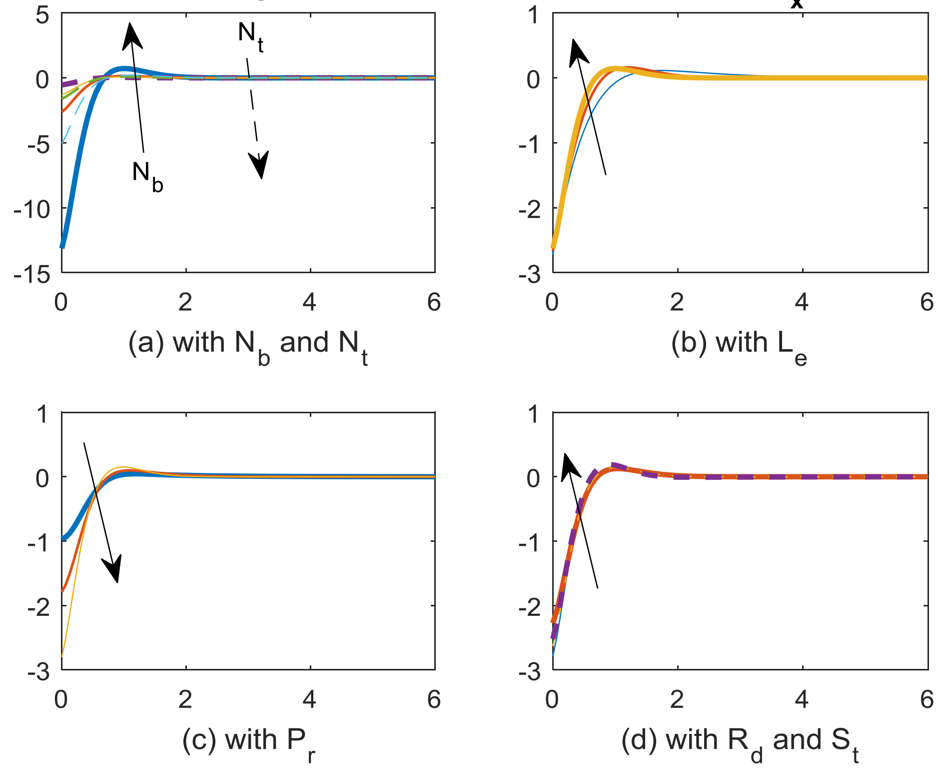

REFERENCES

1. *S. Choi, "Enhancing conductivity of fluids with nanoparticles, ASME Fluid Eng," Division, vol. 231, pp. 99-105, 1995.*
2. *B. M'hamed, N. A. C. Sidik, M. N. A. W. M. Yazid, R. Mamat, G. Najafi, and G. Kefayati, "A review on why researchers apply external magnetic field on nanofluids," International Communications in Heat and Mass Transfer, vol. 78, pp. 60-67, 2016.*
3. *T. Hayat, M. Waqas, S. Shehzad, and A. Alsaedi, "A model of solar radiation and Joule heating in magnetohydrodynamic (MHD) convective flow of thixotropic nanofluid," Journal of Molecular Liquids, vol. 215, pp. 704-710, 2016.*
4. *R. Kandasamy, R. Mohammad, N. A. B. M. Zailani, and N. F. B. Jaafar, "Nanoparticle shapes on squeezed MHD nanofluid flow over a porous sensor surface," Journal of Molecular Liquids, vol. 233, pp. 156-165, 2017.*
5. *R. Kumar, S. Sood, M. Sheikholeslami, and S. A. Shehzad, "Nonlinear thermal radiation and cubic autocatalysis chemical reaction effects on the flow of stretched nanofluid under rotational oscillations," Journal of Colloid and Interface Science, 2017.*
6. *Y. S. Daniel, "Presence of heat generation/absorption on boundary layer slip flow of nanofluid over a porous stretching sheet," American J. of Heat and Mass Transfer, vol. 2, no. 1, p. 15, 2015.*
7. *M. M. Bhatti, T. Abbas, and M. M. Rashidi, "Entropy generation as a practical tool of optimisation for non-Newtonian nanofluid flow through a permeable stretching surface using SLM," Journal of Computational Design and Engineering, vol. 4, no. 1, pp. 21-28, 2017.*
8. *T. Hayat, F. Shah, A. Alsaedi, and M. I. Khan, "Development of homogeneous/heterogeneous reaction in flow based through non-Darcy Forchheimer medium," Journal of Theoretical and Computational Chemistry, p. 1750045, 2017.*
9. *T. Hayat, M. W. A. Khan, A. Alsaedi, and M. I. Khan, "Squeezing flow of second grade liquid subject to non-Fourier heat flux and heat generation/absorption," Colloid and Polymer Science, vol. 295, no. 6, pp. 967-975, 2017.*
10. *M. I. Khan, T. Hayat, M. I. Khan, and A. Alsaedi, "A modified homogeneous/heterogeneous reactions for MHD stagnation flow with viscous dissipation and Joule heating," International Journal of Heat and Mass Transfer, vol. 113, pp. 310-317, 2017.*
11. *T. Fang, J. Zhang, and Y. Zhong, "Boundary layer flow over a stretching sheet with variable thickness," Applied Mathematics and Computation, vol. 218, no. 13, pp. 7241- 7252, 2012.*
12. *T. Hayat, M. I. Khan, M. Farooq, A. Alsaedi, M. Waqas, and T. Yasmeen, "Impact of Cattaneo–Christov heat flux model in flow of variable thermal conductivity fluid over a variable thicked surface," International Journal of Heat and Mass Transfer, vol. 99, pp. 702-710, 2016.*
13. *T. Hayat, M. I. Khan, A. Alsaedi, and M. I. Khan, "Homogeneous-heterogeneous reactions and melting heat transfer effects in the MHD flow by a stretching surface with variable thickness," Journal of Molecular Liquids, vol. 223, pp. 960-968, 2016.*
14. *M. I. Khan, M. I. Khan, M. Waqas, T. Hayat, and A. Alsaedi, "Chemically reactive flow of Maxwell liquid due to variable thicked surface," International Communications in Heat and Mass Transfer, vol. 86, pp. 231-238, 2017.*
15. *M. W. A. Khan, M. Waqas, M. I. Khan, A. Alsaedi, and T. Hayat, "MHD stagnation point flow accounting variable thickness and slip conditions," Colloid and Polymer Science, pp. 1-9, 2017.*
16. *M. Waqas, M. I. Khan, T. Hayat, A. Alsaedi, and M. I. Khan, "Nonlinear thermal radiation in flow induced by a slendering surface accounting thermophoresis and Brownian diffusion," The European Physical Journal Plus, vol. 132, no. 6, p. 280, 2017.*
17. *M. I. Khan, T. Hayat, M. Waqas, M. I. Khan, and A. Alsaedi, "Impact of heat generation/absorption and homogeneous-heterogeneous reactions on flow of Maxwell fluid," Journal of Molecular Liquids, vol. 233, pp. 465-470, 2017.*
18. *M. Waqas, M. Farooq, M. I. Khan, A. Alsaedi, T. Hayat, and T. Yasmeen, "Magnetohydrodynamic (MHD) mixed convection flow of micropolar liquid due to nonlinear stretched sheet with convective condition," International Journal of Heat and Mass Transfer, vol. 102, pp. 766-772, 2016.*
19. *T. Hayat, M. Waqas, M. I. Khan, and A. Alsaedi, "Analysis of thixotropic nanomaterial in a doubly stratified medium considering magnetic field effects," International Journal of Heat and Mass Transfer, vol. 102, pp. 1123-1129, 2016.*
20. *T. Hayat, M. I. Khan, M. Waqas, T. Yasmeen, and A. Alsaedi, "Viscous dissipation effect in flow of magnetonanofluid with variable properties," Journal of Molecular Liquids, vol. 222, pp. 47-54, 2016.*
21. *T. Hayat, M. I. Khan, M. Waqas, A. Alsaedi, and T. Yasmeen, "Diffusion of chemically reactive species in third grade fluid flow over an exponentially stretching sheet considering magnetic field effects," Chinese Journal of Chemical Engineering, vol. 25, no. 3, pp. 257-263, 2017.*
22. *M. I. Khan, M. Kiyani, M. Malik, T. Yasmeen, M. W. A. Khan, and T. Abbas, "Numerical investigation of magnetohydrodynamic stagnation point flow with variable properties," Alexandria Engineering Journal, vol. 55, no. 3, pp. 2367-2373, 2016.*
23. *A. Alsaedi, M. I. Khan, M. Farooq, N. Gull, and T. Hayat, "Magnetohydrodynamic (MHD) stratified bioconvective flow of nanofluid due to gyrotactic microorganisms," Advanced Powder Technology, vol. 28, no. 1, pp. 288-298, 2017.*
24. *T. Hayat, M. Waqas, M. I. Khan, and A. Alsaedi, "Impacts of constructive and destructive chemical reactions in magnetohydrodynamic (MHD) flow of Jeffrey liquid due to nonlinear radially stretched surface," Journal of Molecular Liquids, vol. 225, pp. 302-310, 2017.*
25. *Y. S. Daniel, "Steady MHD Laminar Flows and Heat Transfer Adjacent to Porous Stretching Sheets using HAM," American Journal of Heat and Mass Transfer, vol. 2, no. 3, pp. 146-159, 2015.*
26. *Y. S. Daniel, "MHD Laminar Flows and Heat Transfer Adjacent to Permeable Stretching Sheets with Partial Slip Condition," Journal of Advanced Mechanical Engineering, vol. 4, no. 1, pp. 1-15, 2017.*
27. *Y. S. Daniel, "Steady MHD Boundary-layer Slip Flow and Heat Transfer of Nanofluid over a Convectively Heated of a Non-linear Permeable Sheet," Journal of Advanced Mechanical Engineering, vol. 3, no. 1, pp. 1-14, 2016.*
28. *Y. S. Daniel, "Laminar Convective Boundary Layer Slip Flow over a Flat Plate using Homotopy Analysis Method," Journal of The Institution of Engineers (India): Series E, vol. 97, no. 2, pp. 115-121, 2016.*

29. *R. S. Raju, G. J. Reddy, J. A. Rao, and M. Rashidi, "Thermal diffusion and diffusion thermo effects on an unsteady heat and mass transfer magnetohydrodynamic natural convection Couette flow using FEM," Journal of Computational Design and Engineering, vol. 3, no. 4, pp. 349-362, 2016.*
30. *K. Das, R. P. Sharma, and A. Sarkar, "Heat and mass transfer of a second grade magnetohydrodynamic fluid over a convectively heated stretching sheet," Journal of Computational Design and Engineering, vol. 3, no. 4, pp. 330-336, 2016.*
31. *M. Sheikholeslami and S. Shehzad, "Magnetohydrodynamic nanofluid convection in a porous enclosure considering heat flux boundary condition," International Journal of Heat and Mass Transfer, vol. 106, pp. 1261-1269, 2017.*
32. *M. Sheikholeslami and S. Shehzad, "CVFEM for influence of external magnetic source on Fe_3O_4-H_2O nanofluid behavior in a permeable cavity considering shape effect," International Journal of Heat and Mass Transfer, vol. 115, pp. 180-191, 2017.*
33. *T. Hayat, S. Qayyum, S. A. Shehzad, and A. Alsaedi, "Simultaneous effects of heat generation/absorption and thermal radiation in magnetohydrodynamics (MHD) flow of Maxwell nanofluid towards a stretched surface," Results in Physics, vol. 7, pp. 562-573, 2017.*
34. *T. Hussain, S. Shehzad, T. Hayat, and A. Alsaedi, "Hydromagnetic flow of third grade nanofluid with viscous dissipation and flux conditions," AIP Advances, vol. 5, no. 8, 2015.*
35. *Y. S. Daniel, Z. A. Aziz, Z. Ismail, and F. Salah, "Effects of thermal radiation, viscous and Joule heating on electrical MHD nanofluid with double stratification," Chinese Journal of Physics, vol. 55, no. 3, pp. 630-651, 2017.*
36. *P. Besthapu, R. U. Haq, S. Bandari, and Q. M. Al-Mdallal, "Mixed convection flow of thermally stratified MHD nanofluid over an exponentially stretching surface with viscous dissipation effect," Journal of the Taiwan Institute of Chemical Engineers, vol. 71, pp. 307-314, 2017.*
37. *M. Malik, S. Bilal, M. Bibi, and U. Ali, "Logarithmic and parabolic curve fitting analysis of dual stratified stagnation point MHD mixed convection flow of Eyring-Powell fluid induced by an inclined cylindrical stretching surface," Results in Physics, vol. 7, pp. 544- 552, 2017.*
38. *T. Hayat, M. Rashid, M. Imtiaz, and A. Alsaedi, "MHD effects on a thermo-solutal stratified nanofluid flow on an exponentially radiating stretching sheet," Journal of Applied Mechanics and Technical Physics, vol. 58, no. 2, pp. 214-223, 2017.*
39. *T. Hayat, A. Nassem, M. I. Khan, M. Farooq, and A. Al-Saedi, "Magnetohydrodynamic (MHD) flow of nanofluid with double stratification and slip conditions," Physics and Chemistry of Liquids, pp. 1-20, 2017.*
40. *A. Kuznetsov and D. Nield, "The Cheng–Minkowycz problem for natural convective boundary layer flow in a porous medium saturated by a nanofluid: a revised model," International Journal of Heat and Mass Transfer, vol. 65, pp. 682-685, 2013.*
41. *P. K. Pattnaik and T. Biswal ,MHD free convective boundary layer flow of a viscous fluid at a vertical surface through porous media with non-uniform heat source,IJISET,2(3)(2015).*
42. *P. K. Pattnaik, T. Biswal, Analytical Solution of MHD Free Convective Flow through Porous Media with Time Dependent Temperature and Concentration, Walailak J Sci & Tech, 12 (9) (2015) 749-762.*
43. *P. K. Pattnaik, S R Mishra, , Bhatti M M, Abbas T, Analysis of heat and mass transfer with MHD and chemical reaction effects on viscoelastic fluid over a stretching sheet, Indian J Phys(2017), DOI 10.1007/s12648-017-1022-2.*
44. *P. K. Pattnaik, Mishra S R, Dash G C, Effect of heat source and double stratification on MHD free convection in a micropolar fluid, Alexandria Engineering Journal, 54 (2015) 681–689.*
45. *P. K. Pattnaik, N. Mishra, M. M. Muduly, N. B. Mohapatra, Effect Of Chemical Reaction On Nanofluid Flow Over An Unsteady Stretching Sheet In Presence Of Heat Source, Pramana Research Journal, 8 (8) (2018)142-166.*
46. *T. Hayat, M. I. Khan, M. Farooq, T. Yasmeen, and A. Alsaedi, "Stagnation point flow with Cattaneo-Christov heat flux and homogeneous-heterogeneous reactions," Journal of Molecular Liquids, vol. 220, pp. 49-55, 2016.*
47. *M. I. Khan, T. Hayat, M. Waqas, and A. Alsaedi, "Outcome for chemically reactive aspect in flow of tangent hyperbolic material," Journal of Molecular Liquids, vol. 230, pp. 143-151, 2017.*
48. *M. I. Khan, M. Waqas, T. Hayat, and A. Alsaedi, "A comparative study of Casson fluid with homogeneous-heterogeneous reactions," Journal of Colloid and Interface Science, vol. 498, pp. 85-90, 2017.*
49. *T. Hayat, M. I. Khan, M. Waqas, and A. Alsaedi, "Mathematical modeling of non-Newtonian fluid with chemical aspects: a new formulation and results by numerical technique," Colloids and Surfaces A: Physicochemical and Engineering Aspects, vol. 518, pp. 263-272, 2017.*
50. *M.Q. Brewster, Thermal Radiative Transfer Properties, Wiley, New York, (1972).*
51. *T. Cebeci and P. Bradshaw, Physical and computational aspects of convective heat transfer. Springer Science & Business Media, 2012.*